

Tumor Interstitial Fluid Pressure—A Link between Tumor Hypoxia, Microvascular Density, and Lymph Node Metastasis

Einar K. Rofstad, Kanthi Galappathi and Berit S. Mathiesen

Department of Radiation Biology, Institute for Cancer Research, Oslo University Hospital, Oslo, Norway

Abstract

High microvascular density (MVD) in the primary tumor has been shown to be associated with increased incidence of lymph node metastases and poor clinical outcome. Other investigations have revealed that a large fraction of hypoxic tissue in the primary tumor is associated with metastatic disease and impaired survival. These data are apparently incompatible because tumor hypoxia is primarily a consequence of poor oxygen supply caused by an inadequate vasculature with increased intervessel distances. Here, we provide an explanation of these observations. Human melanoma xenografts were used as preclinical cancer models. Tumors that metastasized to lymph nodes showed higher interstitial fluid pressure (IFP) than those that did not metastasize, and compared with tumors with low IFP, tumors with high IFP showed large hypoxic fractions centrally, high MVD in the periphery, high peritumoral density of lymphatics, and elevated expression of vascular endothelial growth factor A (VEGF-A) and VEGF-C. Significant correlations were found between peripheral MVD and central hypoxia, and lymph node metastasis was associated with high values of both parameters. These findings suggest that the outcome of cancer may be associated with both high MVD and extensive hypoxia in the primary tumor. We propose that proangiogenic factors are upregulated in the tumor center and that the outward interstitial fluid flow caused by the elevated IFP transports these factors to the tumor surface where they evoke hemangiogenesis and lymphangiogenesis, and consequently, that the IFP serves as a link between tumor hypoxia, peripheral tumor hemangiogenesis, peritumoral lymphangiogenesis, and lymph node metastasis.

Neoplasia (2014) 16, 586–594

Introduction

Angiogenesis plays an important role in the progression of malignant diseases [1], and there is substantial evidence that the prognosis

of patients with cancer is associated with the angiogenic potential of the primary tumor [2–4]. Clinical studies involving a wide range of cancer types have demonstrated significant correlations between disease-free or overall survival rate and tumor microvascular density (MVD) [4]. Furthermore, tumor MVD has been shown to be significantly higher in patients with metastases than in metastasis-free patients in many cancer diseases, including breast carcinoma [5], prostate carcinoma [6], squamous cell carcinoma of the head and neck [7], lung carcinoma [8], bladder carcinoma [9], ovarian carcinoma [10], and malignant melanoma [11–13]. Interestingly, most of these cancer types metastasize to regional lymph nodes through functional lymphatics adjacent to the primary tumor, whereas MVD was scored by determining the density of blood vessels in vascular hot spots within the primary tumor [4]. Vascular hot spots can occur anywhere in tumors but are seen primarily in the invasive front [14], consistent with the observation that MVD increases gradually from the center to the periphery of tumors [15].

Abbreviations: HF, hypoxic fraction; IFP, interstitial fluid pressure; LVD, lymph vessel density; LYVE-1, lymphatic endothelial hyaluronan receptor-1; MVD, microvascular density; VEGF, vascular endothelial growth factor

Address all correspondence to: Einar K. Rofstad PhD, Department of Radiation Biology, Institute for Cancer Research, Norwegian Radium Hospital, Box 4953 Nydalen, N-0424 Oslo, Norway. E-mail: enar.k.rofstad@rr-research.no

Financial support was received from the Norwegian Cancer Society and the South-Eastern Norway Regional Health Authority. Conflicts of interest: The authors have no conflicts of interest to disclose.

Received 12 June 2014; Revised 8 July 2014; Accepted 11 July 2014

© 2014 Neoplasia Press, Inc. Published by Elsevier Inc. This is an open access article under the CC BY-NC-ND license (<http://creativecommons.org/licenses/by-nc-nd/3.0/>).

<http://dx.doi.org/10.1016/j.neo.2014.07.003>

The microvascular networks of most tumors have significant morphologic and architectural abnormalities [16–18]. These abnormalities result in elevated geometric and viscous resistance to blood flow, increased transvascular fluid flow, inadequate perfusion, and heterogeneous supply of oxygen and nutrients [16,17]. Therefore, many macroscopic tumors show a physiological microenvironment characterized by nutrient deprivation, high interstitial fluid pressure (IFP), and hypoxia [17,18]. There is significant evidence that these abnormalities promote metastatic dissemination and tumor growth at regional and distant sites [18,19]. Several preclinical studies have suggested that tumors with high fractions of hypoxic cells metastasize more frequently than genetically equivalent tumors with low hypoxic fractions (HFs) [20–24], and highly elevated IFP has been shown to be associated with increased incidence of pulmonary and lymph node metastases in human melanoma and cervical carcinoma xenografts [25,26]. Clinical investigations have revealed that extensive hypoxia in the primary tumor is associated with malignant progression, development of metastatic disease, and poor disease-free and overall survival rates in a large number of cancer types [27–30]. Studies of patients with locally advanced cervical carcinoma have suggested that high IFP in the primary tumor is linked to high incidence of distant metastases, pelvic recurrence after radiation therapy, and impaired survival [31,32].

Large HFs in tumors and hypoxia-induced resistance to radiation therapy have been shown to be associated with low tumor MVD in several cancer types, including cervical carcinoma [33] and carcinoma of the head and neck [34], consistent with the generally accepted view that tumor hypoxia is primarily a consequence of poor oxygen supply caused by elevated resistance to blood flow and increased intervessel distances [17,18]. The significant number of studies suggesting that lymph node metastasis and poor survival rates are associated with high tumor MVD is apparently inconsistent with those suggesting that metastasis and poor outcome are a consequence of tumor hypoxia. It has been proposed, however, that high MVD may result from hypoxia-induced angiogenesis mediated by proangiogenic factors that are upregulated by hypoxia and, hence, that the two sets of apparently inconsistent observations are not mutually exclusive. Although hypoxia-induced angiogenesis may be important, this is not a satisfactory explanation because hypoxic tissue usually exists in the central regions of tumors [17], whereas high MVD and microvascular hot spots are seen primarily in the tumor periphery [14].

In the work reported in this communication, possible relationships between tumor hypoxia, intratumoral MVD, and lymph node metastasis were studied by using human melanoma xenografts as experimental models of human cancer. The main purpose of the study was to provide plausible explanations for 1) the observations that cancer metastasis may be associated with both the fraction of hypoxic tissue and the MVD of the primary tumor and 2) the observations that the density of blood vessels within primary tumors may be associated with lymphogenous metastatic spread. We hypothesized that the elevated IFP and the associated interstitial fluid flow of tumors may serve as a link between tumor hypoxia, MVD, and lymph node metastasis. This hypothesis was investigated by measuring the central IFP, the central fraction of hypoxic tissue, and the peripheral MVD of metastatic and non-metastatic R-18 and T-22 tumors and relating the observations to established correlations between IFP, rate of interstitial fluid flow, and lymph node metastasis.

Materials and Methods

Mice

Adult (8–10 weeks of age) female BALB/c *nu/nu* mice, bred and maintained under specific pathogen-free conditions, were used as host animals for tumors. The animal experiments were approved by the Institutional Committee on Research Animal Care and were done according to the US Public Health Service Policy on Humane Care and Use of Laboratory Animals.

Tumors

The R-18 and T-22 human melanoma cell lines were established in our laboratory as described earlier [35]. The cells used in the present experiments were obtained from our frozen stock and were maintained in monolayer culture in Roswell Park Memorial Institute 1640 (25 mmol/l HEPES and L-glutamine) medium supplemented with 13% bovine calf serum, 250 mg/l penicillin, and 50 mg/l streptomycin. Xenografted tumors were initiated by inoculating aliquots of $\sim 3.5 \times 10^5$ R-18 cells or $\sim 1.0 \times 10^6$ T-22 cells intradermally into the left mouse flank. The tumors were included in experiments when they had grown to a volume of $\sim 400 \text{ mm}^3$. R-18 and T-22 tumors of this size do not show significant regions with necrotic tissue.

Hypoxia, Density of Blood and Lymph Vessels, and Expression of Vascular Endothelial Growth Factor A and Vascular Endothelial Growth Factor C

Hypoxic tissue, blood vessels, lymphatics, vascular endothelial growth factor A (VEGF-A), and VEGF-C were detected by immunohistochemistry [36]. Pimonidazole [1-[(2-hydroxy-3-piperidinyl)-propyl]-2-nitroimidazole], injected as described previously [23], was used as a marker of tumor hypoxia, and CD31 and lymphatic endothelial hyaluronan receptor-1 (LYVE-1) were used as markers of blood and lymph vessel endothelial cells, respectively. An anti-pimonidazole rabbit polyclonal antibody (Professor Raleigh, University of North Carolina, Chapel Hill, NC), an anti-mouse CD31 rat monoclonal antibody (Research Diagnostics, Flanders, NJ), an anti-mouse LYVE-1 rabbit polyclonal antibody (Abcam, Cambridge, United Kingdom), an anti-human VEGF-A rabbit polyclonal antibody (Santa Cruz Biotechnology, Santa Cruz, CA), or an anti-human VEGF-C goat polyclonal antibody (Abcam) was used as primary antibody. Quantitative studies were carried out on preparations cut sagittally through the central regions of tumors and the surrounding skin, and four sections were analyzed for each tumor. Microvessels were defined and scored manually as described by Weidner [14]. Blood vessel density in the invasive front (peripheral MVD) was determined by counting vessels located within a 1-mm-thick band in the tumor periphery (Figure 1, A and B). Peritumoral density of lymphatics [peritumoral lymph vessel density (LVD)] was assessed by counting vessels in the surrounding skin located within a distance of 0.5 mm from the tumor surface. Fraction of hypoxic tissue was assessed by image analysis and was defined as the area fraction of the tissue showing positive pimonidazole staining. HF in the tumor center (central HF_{rim}) was measured by analyzing the tissue located inside the invasive front, that is, further in from the tumor surface than 1 mm (Figure 1, A and B).

VEGF-A Concentration

VEGF-A concentrations were measured in tumors frozen in liquid nitrogen immediately after resection [37]. The frozen tissue was pulverized and lysed in radioimmunoprecipitation assay buffer. The samples were centrifuged and the supernatants were stored at -80°C until analysis. Total protein concentrations were determined by using

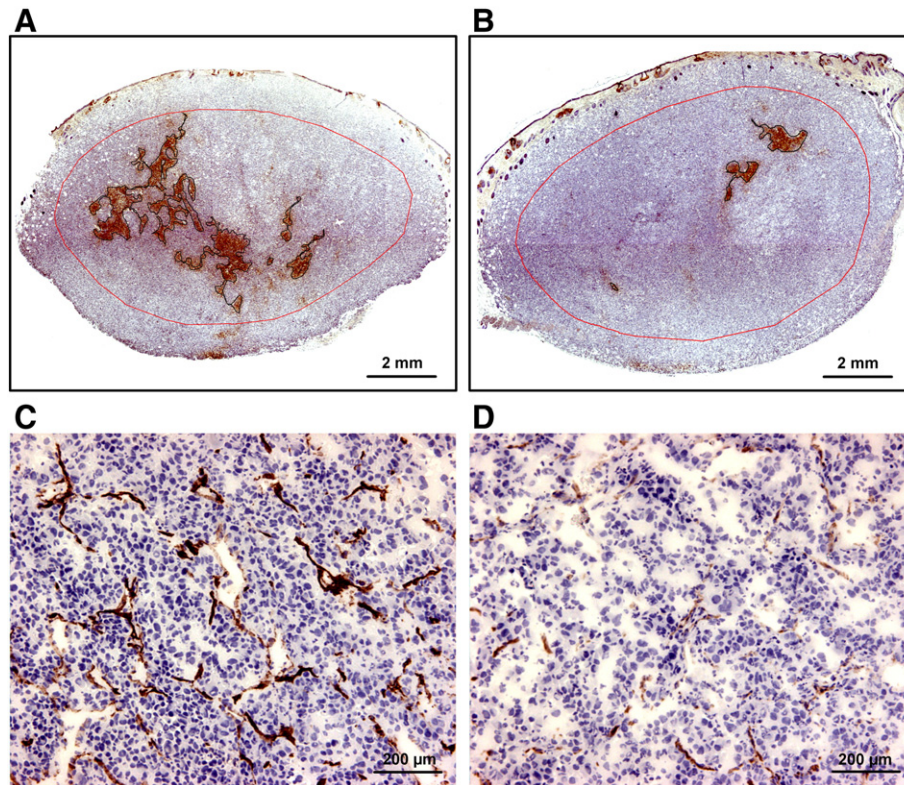


Figure 1. (A and B) Immunohistochemical preparations of two T-22 tumors stained for the hypoxia marker pimonidazole, one with a high HF (A) and the other with a low HF (B). The red lines indicate the border between the peripheral and central tumor regions. (C and D) Immunohistochemical preparations of the peripheral (C) and central (D) regions of the tumor in (A) stained for CD31.

a standard method (BCA assay; Perbio, Rockford, IL). A commercial ELISA kit (Quantikine; R&D Systems, Abingdon, United Kingdom) was used according to the manufacturer's protocol to measure VEGF-A concentrations, and the resulting concentrations were normalized by the total protein concentration.

Interstitial Fluid Pressure

IFP was measured in the center of tumors by using the wick-in-needle method [37]. Before measurements, the host mice were anesthetized with 0.63 mg/kg fentanyl citrate (Janssen Pharmaceutica, Beerse, Belgium), 20 mg/kg fluanisone (Janssen Pharmaceutica), and 10 mg/kg midazolam (Hoffmann-La Roche, Basel, Switzerland).

Lymph Node Metastasis

Spontaneous metastasis was studied as described elsewhere [22]. The mice were killed immediately after the IFP measurement, and after the primary tumor was resected, they were examined for external lymph node metastases in the inguinal, axillary, interscapular, and submandibular regions and internal lymph node metastases in the abdomen and mediastinum. The presence of metastatic growth in enlarged lymph nodes was confirmed by histologic examination [23].

Statistical Analysis

Curves were fitted to data by regression analysis. The Pearson product moment correlation test was used to search for correlations between parameters. Statistical comparisons of data were carried out with the Student's *t* test when the data complied with the conditions of normality and equal variance. Under other conditions, comparisons were carried out by nonparametric analysis using the Mann-Whitney

rank-sum test. Probability values of $P < .05$, determined from two-sided tests, were considered significant. The statistical analysis was performed by using the SigmaStat statistical software (SPSS Science, Chicago, IL).

Results

Fraction of hypoxic tissue differed substantially among individual R-18 and T-22 tumors, as illustrated by immunohistochemical preparations of two distinctly different T-22 tumors (Figure 1, A and B). The red line in these images indicates the border between the central and peripheral tumor regions. Positive pimonidazole staining was seen almost exclusively in the central region, both in R-18 and T-22 tumors. Moreover, immunohistochemical preparations stained for CD31 revealed that the tumors of both lines had higher MVD in the peripheral region than in the central region, as illustrated by using the T-22 tumor depicted in Figure 1A as an example (Figure 1, C and D).

IFP, central HF_{Pim}, and peripheral MVD were measured in 20 R-18 tumors (Figure 2A) and 20 T-22 tumors (Figure 2B). In tumors with IFP below ~20 mmHg, central HF_{Pim} and peripheral MVD did not vary with increasing IFP in any of the lines ($P > .05$). In tumors with IFP above ~20 mmHg, however, both lines showed a positive correlation between central HF_{Pim} and IFP [$P = .024$, $R^2 = 0.49$ (R-18); $P = .012$, $R^2 = 0.56$ (T-22)] and between peripheral MVD and IFP [$P = .0027$, $R^2 = 0.69$ (R-18); $P = .011$, $R^2 = 0.57$ (T-22)]. Moreover, regardless of IFP, there was a significant correlation between peripheral MVD and central HF_{Pim} in both R-18 ($P < .00001$, $R^2 = 0.70$) and T-22 ($P < .00001$, $R^2 = 0.73$) tumors.

Nine of the 20 mice with R-18 tumors and 7 of the 20 mice with T-22 tumors developed lymph node metastases, whereas the other mice were metastasis-negative. The metastatic tumors had significantly higher IFP, central HF_{Pim}, and peripheral MVD than the non-

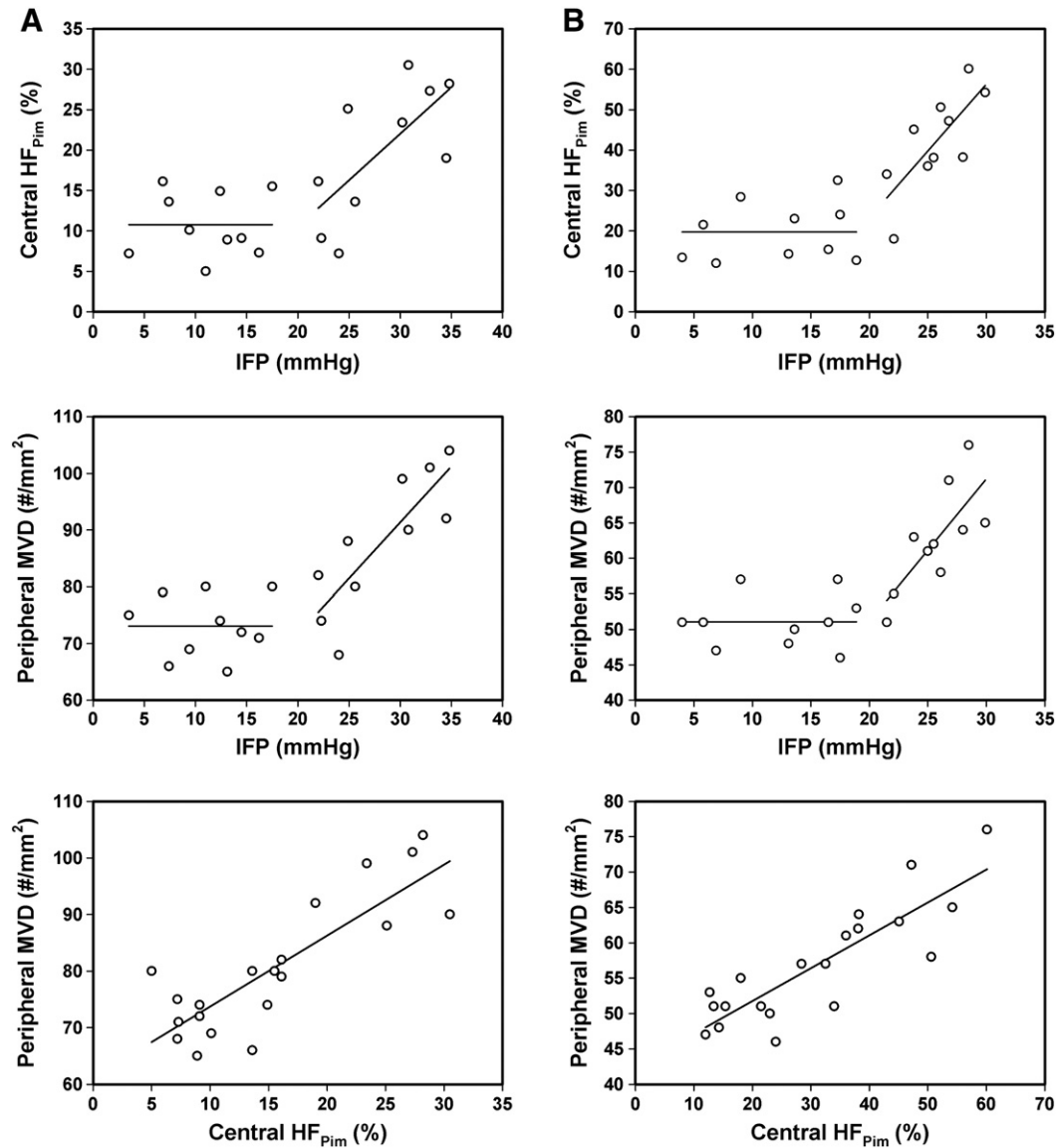


Figure 2. Plots of central HF_{Prim} versus IFP, peripheral MVD versus IFP, and peripheral MVD versus central HF_{Prim} for 20 R-18 (A) and 20 T-22 (B) tumors. The points represent single tumors.

metastatic tumors, both in the R-18 line [$P = .00002$ (IFP), $P = .00055$ (central HF_{Prim}), $P = .0016$ (peripheral MVD); Figure 3A] and the T-22 line [$P = .00097$ (IFP), $P = .0020$ (central HF_{Prim}), $P = .00042$ (peripheral MVD); Figure 3B].

VEGF-A expression, VEGF-C expression, and peritumoral LVD differed between tumors with high IFP (IFP > 20 mmHg) and tumors with low IFP (IFP < 20 mmHg) in both lines. This is illustrated qualitatively in Figure 4, which shows immunohistochemical preparations of two R-18 tumors with highly different IFP stained for VEGF-A (Figure 4A), VEGF-C (Figure 4B), and lymphatics (Figure 4, C and D). The central tumor regions showed relatively homogeneous staining for both VEGF-A and VEGF-C independent of tumor IFP, and the vasculature in the tumor periphery was highlighted by strong VEGF-A staining. The staining intensity centrally was substantially stronger in the tumors with high IFP than in the tumors with low IFP, both for VEGF-A (Figure 4A) and VEGF-C (Figure 4B). Peritumoral lymphatics stained positively for LYVE-1 and were easily identifiable, whereas intratumoral lymphatics could not be detected by LYVE-1 immunohistochemistry

(Figure 4C). The tumors with high IFP generally showed higher peritumoral LVD than the tumors with low IFP (Figure 4D).

The concentration of VEGF-A and peritumoral LVD were measured in eight R-18 and eight T-22 tumors with IFP < 20 mmHg and eight R-18 and eight T-22 tumors with IFP > 20 mmHg. The tumors with high IFP had significantly higher VEGF-A concentration and peritumoral LVD than the tumors with low IFP, both in the R-18 line [$P = .00014$ (VEGF-A concentration), $P = .0039$ (peritumoral LVD); Figure 5A] and the T-22 line [$P = .0024$ (VEGF-A concentration), $P = .00081$ (peritumoral LVD); Figure 5B].

Discussion

High angiogenic activity and a high fraction of hypoxic tissue in the primary tumor have been shown to be associated with high incidence of lymph node metastases, poor outcome of treatment, and decreased survival rates in several histologic types of cancer [2–15,27–30]. In the present communication, we provide experimental evidence that lymphogenous metastasis can be associated with both the HF and the

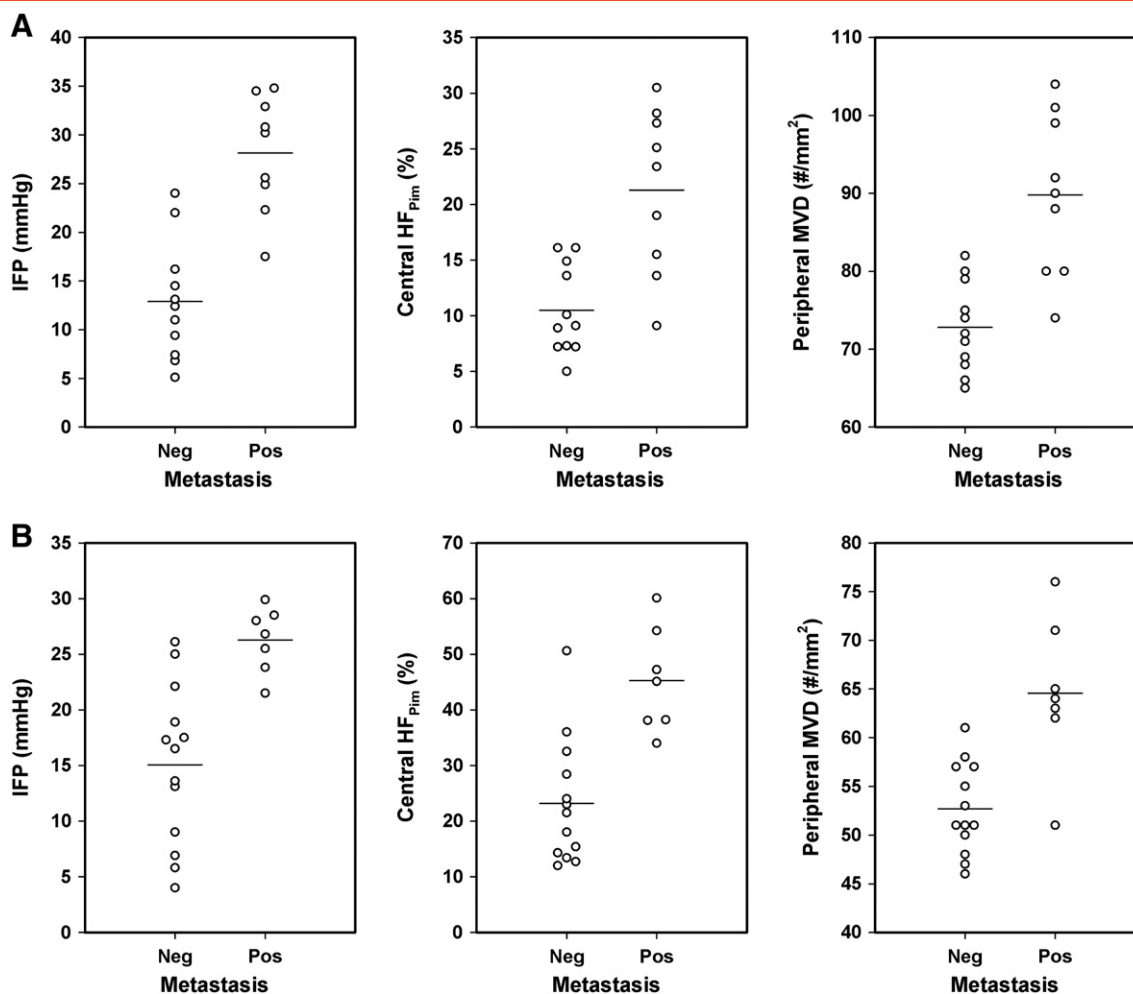


Figure 3. IFP, central HF_{Pim}, and peripheral MVD of nonmetastatic and metastatic R-18 (A) and nonmetastatic and metastatic T-22 (B) tumors. The points represent single tumors. The horizontal lines indicate mean values.

MVD of tumors and suggest a possible mechanism for these apparently incongruous observations.

Human melanoma xenografts growing intradermally in the flank of athymic mice were used as preclinical models of human cancer. Dynamic contrast-enhanced magnetic resonance imaging studies and histologic examinations have revealed that tumors transplanted to this orthotopic site are not isotropic [38]. Blood perfusion and MVD are low in the tumor center and increase toward the periphery in the cranial, dorsal, caudal, and ventral directions, but not in the lateral and medial directions, possibly because any radial gradients in the lateral and medial directions are lost during tumor growth owing to vessel deteriorations caused by mechanical pressure generated by the expanding tumor mass. The histologic sections studied in this investigation were cut in the sagittal plane because vascular gradients appear in all directions in this plane.

Two tumor lines were included in the study, and it was revealed that MVD was higher in the tumor periphery than in the tumor center and that the central regions, in contrast to the peripheral regions, showed significant pimonidazole staining. Moreover, peripheral MVD was positively correlated with central HF_{Pim}, and the metastatic tumors had higher central HF_{Pim} and higher peripheral MVD than the nonmetastatic tumors. Interestingly, the tumors with high IFP (IFP > 20 mmHg) showed higher central HF_{Pim}, higher

peripheral MVD, higher peritumoral LVD, higher expression of VEGF-A and VEGF-C, and metastasized more frequently to lymph nodes than the tumors with low IFP (IFP < 20 mmHg).

Based on these data, we suggest that tumor IFP forms a link between tumor angiogenesis, tumor hypoxia, and lymph node metastasis and that the following mechanism was responsible for our observations. Abnormal angiogenesis led to the development of microvascular networks with severe architectural abnormalities, and these abnormalities resulted in a physiological microenvironment centrally in the tumors characterized by elevated IFP and regions with hypoxic tissue. Tumor hypoxia and interstitial hypertension caused up-regulation of VEGF-A, VEGF-C, and possibly also other stimulators of hemangiogenesis and lymphangiogenesis. Because of the elevated IFP in the central tumor regions, interstitial fluid flowed from the center toward the periphery and transported these proangiogenic factors to the tumor surface where they promoted tumor hemangiogenesis and peritumoral lymphangiogenesis, and subsequently, lymph node metastasis increased because of increased VEGF-C-mediated lymphangiogenesis in the peritumoral tissue.

The different steps of the suggested mechanism are in accordance with the current literature. Thus, there is substantial evidence from preclinical studies that tumor hypoxia and interstitial hypertension are caused primarily by microvascular abnormalities [17,18,39] and

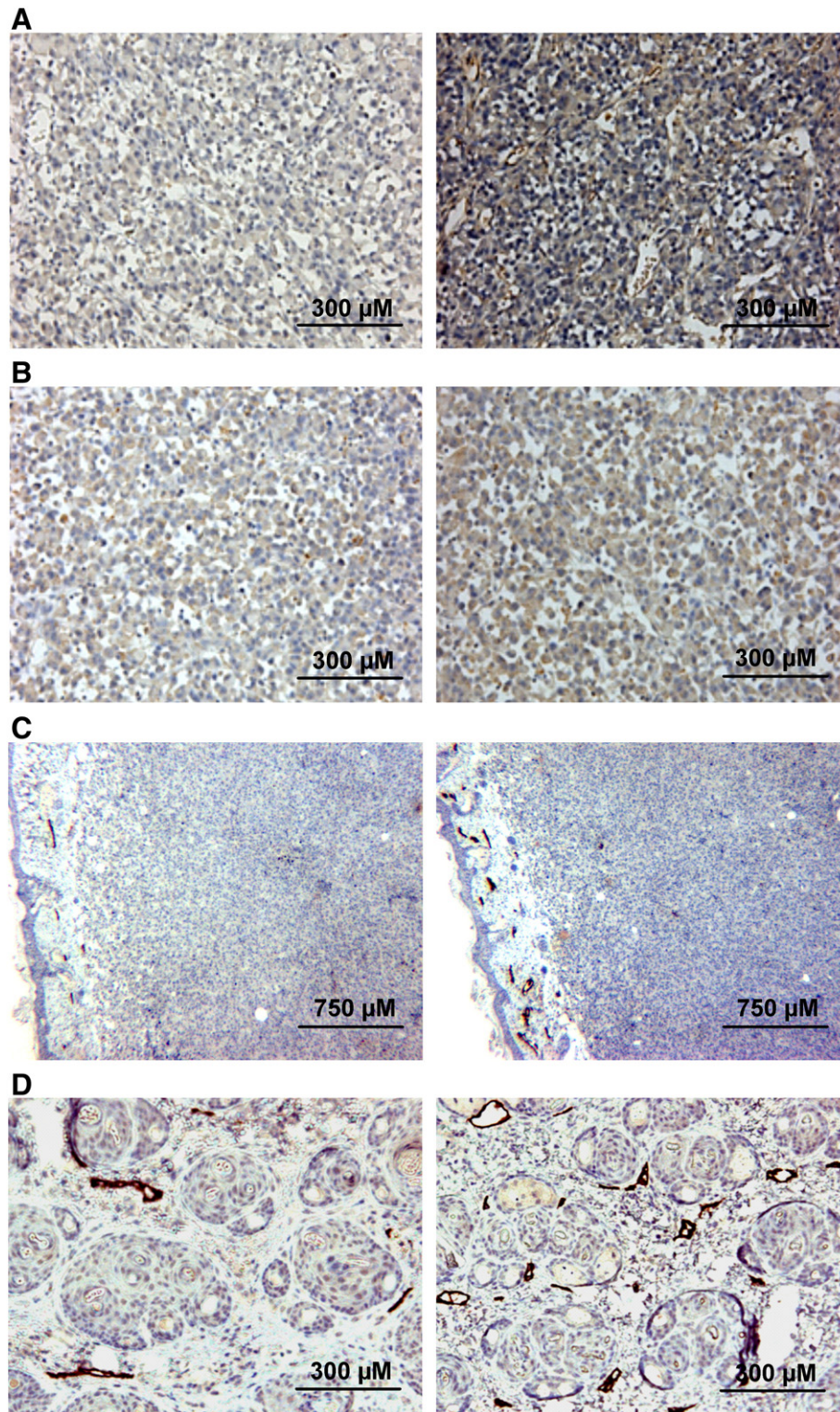


Figure 4. Immunohistochemical preparations of two R-18 tumors stained for VEGF-A (A), VEGF-C (B), and LYVE-1 (C) and of the peritumoral skin of the tumors stained for LYVE-1 (C and D). Peritumoral lymphatics stained positively for LYVE-1 (C and D), whereas intratumoral lymphatics could not be detected (C). The images to the left refer to a tumor with a low IFP of 7 mmHg and those to the right to a tumor with a high IFP of 31 mmHg.

that tumor hypoxia and interstitial hypertension cause up-regulation of VEGF-A, VEGF-C, and other proangiogenic factors [18,40,41]. Theoretical as well as experimental studies have revealed that IFP is homogeneously elevated throughout the central regions of tumors and drops steeply to normal tissue values at the tumor periphery,

resulting in an outward flow of interstitial fluid at the tumor surface [42–44]. It has been shown that the velocity of the peritumoral interstitial fluid flow correlates positively with IFP and the incidence of lymph node metastases in melanoma and cervical carcinoma xenografts [26]. Furthermore, high peritumoral interstitial fluid flow

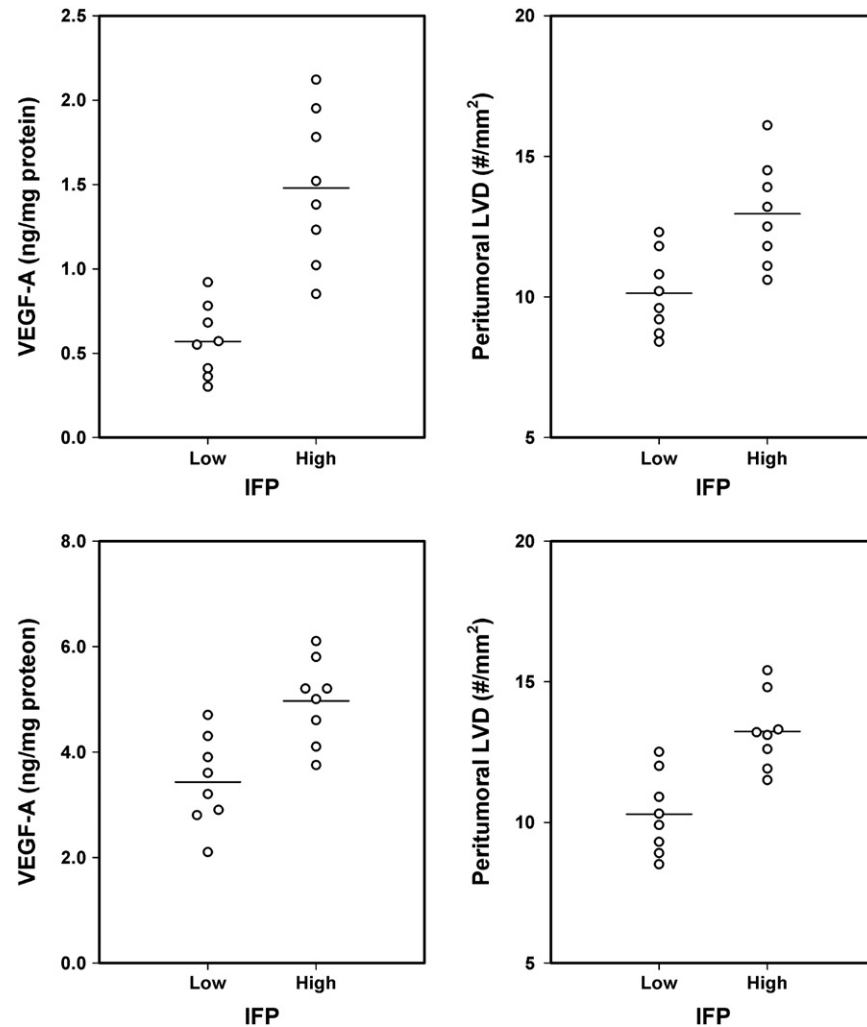


Figure 5. VEGF-A concentration and peritumoral LVD of R-18 (A) and T-22 (B) tumors with low (IFP < 20 mmHg) and high (IFP > 20 mmHg) IFP. The points represent single tumors. The horizontal lines indicate mean values.

velocity has been shown to be associated with lymphogenous metastasis in patients diagnosed with locally advanced carcinoma of the uterine cervix [26].

In addition to microvascular abnormalities, impaired lymphatic drainage has been identified as a key contributor to the development of interstitial hypertension in tumors [45,46], and consequently, the present observation of an association between high IFP and high peritumoral LVD is counterintuitive. Tumor-induced lymphangiogenesis may produce lymphatics with severe morphologic and functional abnormalities, analogous to the observation that tumor hemangiogenesis may result in the development of abnormal blood vessels. Thus, it has been observed that some tumors show overexpression of prolymphangiogenic factors and that these factors may evoke hyperplasia of peritumoral lymphatics and produce immature lymphatics with reduced draining capacity [47,48]. Most likely, the peritumoral lymphangiogenesis induced by VEGF-C in R-18 and T-22 tumors with high IFP was not sufficient to have any impact on the IFP of the tumors, either because the magnitude of the increase in peritumoral LVD was too small or because the functional ability of the lymphatics was subnormal.

Recently, Hofmann et al. [49] studied effects of lymphangiogenesis on tumor IFP by injecting high doses of VEGF-C in the peritumoral

tissue of epidermoid vulva carcinoma xenografts and showed that this VEGF-C treatment resulted in strong intratumoral lymphangiogenesis, distinct lymphatics within the tumor tissue, and decreased IFP. Our finding of an association between high IFP and high peritumoral LVD is apparently contradictory to the observation of Hofmann et al. [49]. However, there is a significant difference between these two studies. Intratumoral lymphatics could not be seen in any of the R-18 and T-22 tumors, regardless of IFP, whereas the VEGF-C treatment used by Hofmann et al. [49] evoked strong intratumoral lymphangiogenesis. It is possible that a significant VEGF-C-induced decrease in the IFP of tumors may require induction of functional lymphatic within the malignant tumor tissue.

Most previous studies have failed to demonstrate a correlation between the IFP of tumors and tumor hypoxia, both in patients with cervical cancer [31] and in experimental tumor models [50–52], whereas in this study, a positive correlation was found between central HF_{pim} and IFP in tumors with IFP > 20 mmHg. Different methods were used to measure hypoxia, and in the previous studies, fraction of hypoxic tissue referred to the total tumor volume. Moreover, the detection of any correlation may have been complicated by a large proportion of tumors with relatively low IFP values. Interestingly, in a previous investigation, we measured IFP values ranging from 2 to

18 mmHg in A-07 melanoma xenografts, and in that study, a positive correlation was found between IFP and fraction of acutely hypoxic cells but not between IFP and fraction of chronically hypoxic cells [53].

In contrast to R-18 and T-22 tumors, tumors of the A-07 line rarely show IFP values above 20 mmHg [25,53], and A-07 tumors generally develop lymph node metastases less frequently than R-18 and T-22 tumors [22,23,25]. For example, in a previous study of A-07 tumors, lymph node metastases were detected in 11 of 50 mice (22%) [25], whereas the incidence of lymph node metastases was 45% for the R-18 tumors and 35% for the T-22 tumors in the present study. However, A-07 tumors develop pulmonary metastases frequently [24,25,36], whereas hematogenous spread to the lungs has not been observed for R-18 and T-22 tumors [22,36]. Furthermore, A-07 tumors have a shorter volume doubling time and a substantially higher MVD than R-18 and T-22 tumors [35]. Taken together, our observations suggest that A-07 tumors are more aggressive than R-18 and T-22 tumors [35], most likely because the synthesis and secretion of the proangiogenic factors VEGF-A and interleukin-8 are manyfold higher in A-07 tumors than in other melanoma xenografts we have studied [36].

The mechanism we suggest here implies that lymph node metastasis was primarily a result of microenvironment-induced activation of peritumoral lymphatics mediated by VEGF-C, but other metastasis-promoting factors transported by the interstitial fluid may have been involved as well. However, there was probably not any causal relationship between lymph node metastasis and peripheral MVD. An association between these parameters was probably observed because the outward flow of interstitial fluid brought VEGF-A and other proangiogenic factors to the tumor surface, but it is not likely that the increased peripheral vascularity played a significant role as an escape route for cells giving rise to lymph node metastases.

In conclusion, this preclinical study shows that lymph node metastasis can be associated with the fraction of hypoxic tissue in the central regions of tumors as well as the MVD in the tumor periphery, probably because interstitial hypertension and the associated interstitial fluid flow act as a link between tumor hypoxia, peripheral tumor angiogenesis, peritumoral lymphangiogenesis, and the development of lymph node metastases. Consequently, the apparently incongruous observations that the clinical outcome of cancer is associated with tumor MVD and with tumor hypoxia are not mutually exclusive.

References

- [1] Folkman J (1995). Angiogenesis in cancer, vascular, rheumatoid and other disease. *Nat Med* **1**, 27–31.
- [2] Vermeulen PB, Gasparini G, Fox SB, Colpaert C, Marson LP, Gion M, Beliën JA, de Waal RM, van Marck E, and Magnani E, et al (2002). Second international consensus on the methodology and criteria of evaluation of angiogenesis quantification in solid human tumours. *Eur J Cancer* **38**, 1564–1579.
- [3] Nico B, Benaglio V, Mangieri D, Maruotti N, Vacca A, and Ribatti D (2008). Evaluation of microvascular density in tumors: pro and contra. *Histol Histopathol* **23**, 601–607.
- [4] Weidner N (2008). Measuring intratumoral microvessel density. *Methods Enzymol* **444**, 305–323.
- [5] Weidner N, Semple JP, Welch WR, and Folkman J (1991). Tumor angiogenesis and metastasis—correlation in invasive breast carcinoma. *N Engl J Med* **324**, 1–8.
- [6] Weidner N, Carroll PR, Flax J, Blumenfeld W, and Folkman J (1993). Tumor angiogenesis correlates with metastasis in invasive prostate carcinoma. *Am J Pathol* **43**, 401–409.
- [7] Gasparini G, Weidner N, Maluta S, Pozza F, Boracchi P, Mezzetti M, Testolin A, and Bevilacqua P (1993). Intratumoral microvessel density and p53 protein: correlation with metastasis in head-and-neck squamous-cell carcinoma. *Int J Cancer* **55**, 739–744.
- [8] Macchiarini P, Fontanini G, Hardin MJ, Squartini F, and Angeletti CA (1992). Relation of neovascularisation to metastasis of non-small-cell lung cancer. *Lancet* **340**, 145–146.
- [9] Jaeger TM, Weidner N, Chew K, Moore DH, Kerschmann RL, Waldman FM, and Carroll PR (1995). Tumor angiogenesis correlates with lymph node metastases in invasive bladder cancer. *J Urol* **154**, 59–71.
- [10] Volm M, Koomagi R, Kaufmann M, Mattern J, and Stämmler G (1996). Microvessel density, expression of proto-oncogenes, resistance-related proteins and incidence of metastases in primary ovarian carcinomas. *Clin Exp Metastasis* **14**, 209–214.
- [11] Graham CH, Rivers J, Kerbel RS, Stankiewicz KS, and White WL (1994). Extent of vascularization as a prognostic indicator in thin (<0.76 mm) malignant melanomas. *Am J Pathol* **145**, 510–514.
- [12] Srivastava A, Laidler P, Davies RP, Horgan K, and Hughes LE (1988). The prognostic significance of tumor vascularity in intermediate-thickness (0.76–4.0 mm thick) skin melanoma. A quantitative histologic study. *Am J Pathol* **133**, 419–423.
- [13] Neitzel LT, Neitzel CD, Magee KL, and Malafa MP (1999). Angiogenesis correlates with metastasis in melanoma. *Ann Surg Oncol* **6**, 70–74.
- [14] Weidner N (1995). Intratumor microvessel density as a prognostic factor in cancer. *Am J Pathol* **147**, 9–19.
- [15] Begum R, Douglas-Jones AG, and Morgan JM (2003). Radial intratumoral increase and correlation of microvessels and proliferation in solid breast carcinoma. *Histopathology* **43**, 244–253.
- [16] Jain RK (1988). Determinants of tumor blood flow: a review. *Cancer Res* **48**, 2641–2658.
- [17] Vaupel P, Kallinowski F, and Okunieff P (1989). Blood flow, oxygen and nutrient supply, and metabolic microenvironment of human tumors: a review. *Cancer Res* **49**, 6449–6465.
- [18] Cairns R, Papandreou I, and Denko N (2006). Overcoming physiologic barriers to cancer treatment by molecularly targeting the tumor microenvironment. *Mol Cancer Res* **4**, 61–70.
- [19] Finger EC and Giaccia AJ (2010). Hypoxia, inflammation, and the tumor microenvironment in metastatic disease. *Cancer Metastasis Rev* **29**, 285–293.
- [20] Cairns RA, Kalliomäki T, and Hill RP (2001). Acute (cyclic) hypoxia enhances spontaneous metastasis of KHT murine tumors. *Cancer Res* **61**, 8903–8908.
- [21] Cairns RA and Hill RP (2004). Acute hypoxia enhances spontaneous lymph node metastasis in an orthotopic murine model of human cervical carcinoma. *Cancer Res* **64**, 2054–2061.
- [22] Rofstad EK, Rasmussen H, Galappathi K, Mathiesen B, Nilsen K, and Graff BA (2002). Hypoxia promotes lymph node metastasis in human melanoma xenografts by up-regulating the urokinase-type plasminogen activator receptor. *Cancer Res* **62**, 1847–1853.
- [23] Rofstad EK, Galappathi K, Mathiesen B, and Ruud EB (2007). Fluctuating and diffusion-limited hypoxia in hypoxia-induced metastasis. *Clin Cancer Res* **13**, 1971–1978.
- [24] Rofstad EK, Gaustad JV, Egeland TAM, Mathiesen B, and Galappathi K (2010). Tumors exposed to acute cyclic hypoxic stress show enhanced angiogenesis, perfusion and metastatic dissemination. *Int J Cancer* **127**, 1535–1546.
- [25] Rofstad EK, Tunheim SH, Mathiesen B, Graff BA, Halsør EF, Nilsen K, and Galappathi K (2002). Pulmonary and lymph node metastasis is associated with primary tumor interstitial fluid pressure in human melanoma xenografts. *Cancer Res* **62**, 661–664.
- [26] Hompland T, Ellingsen C, Øvrebø KM, and Rofstad EK (2012). Interstitial fluid pressure and associated lymph node metastasis revealed in tumors by dynamic contrast-enhanced MRI. *Cancer Res* **72**, 4899–4908.
- [27] Höckel M, Schlenger K, Aral B, Mitze M, Schaffer U, and Vaupel P (1996). Association between tumor hypoxia and malignant progression in advanced cancer of the uterine cervix. *Cancer Res* **56**, 4509–4515.
- [28] Brizel DM, Dodge RK, Clough RW, and Dewhirst MW (1999). Oxygenation of head and neck cancer: changes during radiotherapy and impact on treatment outcome. *Radiother Oncol* **53**, 113–117.
- [29] Nordmark M, Alsner J, Keller J, Nielsen OS, Jensen OM, Horsman MR, and Overgaard J (2001). Hypoxia in human soft tissue sarcomas: adverse impact on survival and no association with p53 mutations. *Br J Cancer* **84**, 1070–1075.
- [30] Vaupel P and Mayer A (2007). Hypoxia in cancer: significance and impact on clinical outcome. *Cancer Metastasis Rev* **26**, 225–239.

- [31] Milosevic M, Fyles A, Hedley D, Pintilie M, Levin W, Manchul L, and Hill R (2001). Interstitial fluid pressure predicts survival in patients with cervix cancer independent of clinical prognostic factors and tumor oxygen measurements. *Cancer Res* **61**, 6400–6405.
- [32] Yeo SG, Kim JS, Cho MJ, Kim KH, and Kim JS (2009). Interstitial fluid pressure as a prognostic factor in cervical cancer following radiation therapy. *Clin Cancer Res* **15**, 6201–6207.
- [33] Awwad HK, el Naggat M, Mocktar N, and Barsoum M (1986). Inter-capillary distance measurement as an indicator of hypoxia in carcinoma of the cervix uteri. *Int J Radiat Oncol Biol Phys* **12**, 1329–1333.
- [34] Jenssen N, Boysen M, Kjaerheim A, and Bryne M (1996). Low vascular density indicates poor response to radiotherapy in small glottic carcinomas. *Pathol Res Pract* **192**, 1090–1094.
- [35] Rofstad EK and Mathiesen B (2010). Metastasis in melanoma xenografts is associated with tumor microvascular density rather than extent of hypoxia. *Neoplasia* **12**, 889–898.
- [36] Rofstad EK and Halsør EF (2000). Vascular endothelial growth factor, interleukin 8, platelet-derived endothelial cell growth factor, and basic fibroblast growth factor promote angiogenesis and metastasis in human melanoma xenografts. *Cancer Res* **60**, 4932–4938.
- [37] Rofstad EK, Ruud EBM, Mathiesen B, and Galappathi K (2010). Associations between radiocurability and interstitial fluid pressure in human tumor xenografts without hypoxic tissue. *Clin Cancer Res* **16**, 936–945.
- [38] Gaustad JV, Benjaminsen IC, Graff BA, Brurberg KG, Ruud EB, and Rofstad EK (2005). Intratumor heterogeneity in blood perfusion in orthotopic human melanoma xenografts assessed by dynamic contrast-enhanced magnetic resonance imaging. *J Magn Reson Imaging* **21**, 792–800.
- [39] Lunt SJ, Fyles A, Hill RP, and Milosevic M (2008). Interstitial fluid pressure in tumors: therapeutic barrier and biomarker of angiogenesis. *Future Oncol* **4**, 793–802.
- [40] Rankin EB and Giaccia AJ (2008). The role of hypoxia-inducible factors in tumorigenesis. *Cell Death Differ* **15**, 678–685.
- [41] Nathan SS, Huvos AG, Casas-Ganem JE, Yang R, Linkov I, Sowers R, DiResta GR, Gorlick R, and Healey JH (2008). Tumor interstitial fluid pressure may regulate angiogenic factors in osteosarcoma. *J Orthop Res* **26**, 1520–1525.
- [42] Boucher Y, Baxter LT, and Jain RK (1990). Interstitial pressure gradients in tissue-isolated and subcutaneous tumors: implications for therapy. *Cancer Res* **50**, 4478–4484.
- [43] Milosevic MF, Fyles AW, and Hill RP (1999). The relationship between elevated interstitial fluid pressure and blood flow in tumors: a bioengineering analysis. *Int J Radiat Oncol Biol Phys* **43**, 1111–1123.
- [44] Jain RK, Tong RT, and Munn LL (2007). Effect of vascular normalization by antiangiogenic therapy on interstitial hypertension, peritumor edema, and lymphatic metastasis: insights from a mathematical model. *Cancer Res* **67**, 2729–2735.
- [45] Heldin CH, Rubin K, Pietras K, and Östman A (2004). High interstitial fluid pressure—an obstacle in cancer therapy. *Nat Rev Cancer* **4**, 806–813.
- [46] Padera TP, Stoll BR, Tooredman JB, Capen D, di Tomaso E, and Jain RK (2004). Cancer cells compress intratumour vessels. *Nature* **427**, 695.
- [47] Balkwill FR, Capasso M, and Hagemann T (2012). The tumor microenvironment at a glance. *J Cell Sci* **125**, 5591–5596.
- [48] Swartz MA and Lund AW (2012). Lymphatic and interstitial flow in the tumour microenvironment: linking mechanobiology with immunity. *Nat Rev Cancer* **12**, 210–219.
- [49] Hofmann M, Pflanzner R, Zöller NN, Bernd A, Kaufmann R, Thaci D, Bereiter-Hahn J, Hirohata S, and Kippenberger S (2013). Vascular endothelial growth factor C-induced lymphangiogenesis decreases tumor interstitial fluid pressure and tumor growth. *Trans Oncol* **6**, 398–404.
- [50] Boucher Y, Lee I, and Jain RK (1995). Lack of general correlation between interstitial fluid pressure and oxygen partial pressure in solid tumors. *Microvasc Res* **50**, 175–182.
- [51] Tufto I, Lyng H, and Rofstad EK (1996). Interstitial fluid pressure, perfusion rate and oxygen tension in human melanoma xenografts. *Br J Cancer Suppl* **27**, S252–S255.
- [52] Lunt SJ, Kalliomäki TMK, Brown A, Yang VX, Milosevic M, and Hill RP (2008). Interstitial fluid pressure, vascularity and metastasis in ectopic, orthotopic and spontaneous tumours. *BMC Cancer* **8**, 2.
- [53] Rofstad EK, Gaustad JV, Brurberg KG, Mathiesen B, Galappathi K, and Simonsen TG (2009). Radiocurability is associated with interstitial fluid pressure in human tumor xenografts. *Neoplasia* **11**, 1243–1251.